

The nature of the late B-type stars HD 67044 and HD 42035

R. Monier^{1,2} • M. Gebran³ • F. Royer⁴

Abstract While monitoring a sample of apparently slowly rotating superficially normal bright late B and early A stars in the northern hemisphere, we have discovered that HD 67044 and HD 42035, hitherto classified as normal late B-type stars, are actually respectively a new chemically peculiar star and a new spectroscopic binary containing a very slow rotator HD 42035 S with ultra-sharp lines ($v_e \sin i = 3.7 \text{ km s}^{-1}$) and a fast rotator HD 42035 B with broad lines. The lines of Ti II, Cr II, Mn II, Sr II, Y II, Zr II and Ba II are conspicuous features in the high resolution SOPHIE spectrum ($R = 75000$) of HD 67044. The Hg II line at 3983.93 Å is also present as a weak feature. The composite spectrum of HD 42035 is characterised by very sharp lines formed in HD 42035 S superimposed onto the shallow and broad lines of HD 42035 B. These very sharp lines are mostly due to light elements from C to Ni, the only heavy species definitely present are strontium and barium. Selected lines of 21 chemical elements from He up to Hg have been synthesized using model atmospheres computed with ATLAS9 and the spectrum synthesis code SYNSPEC48 including hyperfine structure of various isotopes when relevant. These synthetic spectra have been adjusted to high resolution high signal-to-noise spectra of HD 67044 and HD 42035 S in order to derive abundances of these key elements. HD 67044 is found to have distinct enhancements of Ti, Cr, Mn, Sr,

Y, Zr, Ba and Hg and underabundances in He, C, O, Ca and Sc which shows that this star is not a superficially normal late B-type star, but actually is a new CP star most likely of the HgMn type. HD 42035 S has provisional underabundances of the light elements from C to Ti and overabundances of heavier elements (except for Fe and Sr which are also underabundant) up to barium. These values are lower limits to the actual abundances as we cannot currently place properly the continuum of HD 42035 S. More accurate fundamental parameters and abundances for HD 42035 S and HD 42035 B will be derived if we manage to disentangle their spectra. They will help clarify the status of the two components in this interesting new spectroscopic binary.

Keywords stars: early-type – stars: abundances – stars: chemically peculiar - stars: spectroscopic binary

1 Introduction

We have recently undertaken a spectroscopic survey of all apparently slowly rotating bright early A stars (A0-A1V) and late B stars (B8-B9V) observable from the northern hemisphere. The incentive is to search for rapid rotators seen pole-on or new chemically peculiar B and A stars which have thus far remained unnoticed. This project addresses fundamental questions of the physics of late-B and early-A stars: i) can we find new instances of rapid rotators seen pole-on (other than Vega) and study their physical properties (gradient of temperature across the disk, limb and gravity darkening), ii) is our census of Chemically Peculiar stars complete up to the magnitude limits we adopted ? If not, what are the physical properties of the newly found CP stars?. The abundance results for the A0-A1V sample have been published in Royer et al. (2014). The selection criteria were: a declination higher than

R. Monier

LESIA, UMR 8109, Observatoire de Paris, place J. Janssen, Meudon.

Laboratoire Lagrange, Université de Nice Sophia, Parc Valrose, 06100 Nice, France.

M. Gebran

Department of Physics and Astronomy, Notre Dame University-Louaize, PO Box 72, Zouk Mikael, Lebanon.

F. Royer

GEPI, Observatoire de Paris, place J. Janssen, Meudon, France.

-15° , spectral class A0 or A1 and luminosity class V and IV and magnitudes V brighter than 6.65 and a $v_e \sin i$ less than 65 km s^{-1} . The B8-9 sample employs the same criteria, except for the V magnitude brighter than 7.85 as these B stars are intrinsically brighter in the V band where SOPHIE reaches its maximum efficiency. Most of the stars of that B8-9 sample (40 stars) have been observed in December 2014 with SOPHIE, the échelle high-resolution spectrograph at Observatoire de Haute Provence yielding spectra covering the 3900 \AA – 6800 \AA spectral range over 39 orders at a resolving power $R = 75000$. A careful abundance analysis of the high resolution high signal-to-noise ratio spectra of the A stars sample has allowed to sort out the sample of 47 A stars into 17 chemically normal stars (ie. whose abundances do not depart by more than ± 0.20 dex from solar values), 12 spectroscopic binaries and 13 chemically peculiar stars (CPs) among which five are new CP stars. The status of these new CP stars still needs to be fully specified by spectropolarimetric observations to address their magnetic nature or by exploring new spectral ranges which we had not explored in this first study. Indeed, the abundance analysis of the A stars sample in Royer et al. (2014) relied only on four spectral regions: 4150 – 4300 \AA , 4400 – 4790 \AA , 4920 – 5850 \AA , and 6000 – 6275 \AA , avoiding Balmer lines and atmospheric telluric lines.

We have now started to examine the B9-B8V sample using the full wavelength coverage provided by SOPHIE to search for new Chemically Peculiar stars. We have already reported on the discovery of 4 new HgMn stars (Monier et al. 2015) whose spectra display strong Hg II lines at 3984 \AA and strong Mn II lines. These new HgMn stars are HD 18104, HD 30085, HD 32867, HD 53588. In the process of our analysis of the B9-B8V sample, we have just found that HD 67044, currently classified B8 in SIMBAD, is actually another new CP star, most likely another new HgMn star and that HD 42035, classified B9V, actually is a new spectroscopic binary containing a slow rotator which we will refer to as HD 42035 S (S for "sharp" lines) and a fast rotator, HD 42035 B (B for "broad" lines). A bibliographic query of the CDS for HD 67044 and HD 42035 actually reveals only 4 and 26 publications respectively. Neither HD 67044 nor HD 42035 appear in Cowley's classification (1972) of the bright B8 stars. The purpose of this paper is to report on the detection of strong Ti II, Cr II, Mn II, Sr II, Y II, Zr II, Ba II lines and a weak Hg II line in the spectrum of HD 67044 and perform a line identification of all the very sharp lines of HD 42035 S. We also have determined the abundances of 17 chemical elements for HD 67044 using spectrum synthesis to quantify the enhancements and depletions of these

elements. As several of the lines of HD 42035 S are blended with those of HD 42035 B, we have only been able to derive provisional abundances for HD 42035 S using lines little affected by the fast rotator.

2 Observations and reduction

HD 67044 and HD 42035 have been observed at Observatoire de Haute Provence using the high resolution ($R = 75000$) mode of the SOPHIE échelle spectrograph (Perruchot et al. 2008) in December 2014. The $\frac{S}{N}$ ratio of the spectra are about 130 and 174 at 5500 \AA respectively. The observations log is displayed in Table 1. The data are automatically reduced to produce 1D extracted and wavelength calibrated échelle orders. Each reduced order was normalised separately using a Chebychev polynomial fit with sigma clipping, rejecting points above or below 1σ of the local continuum. Normalized orders were merged together, corrected by the blaze function and resampled into a constant wavelength step of about 0.02 \AA (see Royer et al. 2014, for more details).

The radial velocities of HD 67044 and HD 42035 were derived from cross-correlation techniques, avoiding the Balmer lines and the atmospheric telluric lines. The normalized spectrum was cross-correlated with a synthetic template extracted from the POLLUX database¹ (Palacios et al. 2010) corresponding to the parameters $T_{\text{eff}} = 11000 \text{ K}$, $\log g = 4$ and solar abundances. A parabolic fit of the upper part of the resulting cross-correlation function yields the Doppler shift, which is then used to shift spectra to rest wavelengths. The radial velocities of HD 67044 and HD 42035 are collected in Table 2.

3 The line spectrum of HD 67044

Several spectral regions have been used to establish the chemical peculiarity of HD 67044. First, the red wing of He, which lies in order 3, harbors the Hg II $\lambda 3983.93 \text{ \AA}$ line and several Zr II and Y II lines likely to be strengthened in CP stars. After proper correction for the stellar radial velocity, we found that HD 67044 does show the Hg II 3983.93 \AA line as a feature absorbing about 2%, and also strong lines of Y II at 3982.59 \AA and of Zr II at 3991.13 \AA and 3998.97 \AA . The Y II, Zr II and Hg II lines in the spectral range 3980 to 4000 \AA are displayed in figure 1 together with the synthetic spectrum fitting best this spectral interval. Several other lines of Y II

¹<http://pollux.graal.univ-montp2.fr>

and Zr II are strong absorbers in the spectrum of HD 67044 and have been used to derive the abundances in these elements. Second, we examined the region from 4125 Å to 4145 Å (order 6) for the Si II lines at 4128.054 Å and 4130.894 Å and the Mn II line at 4136.92 Å. In an HgMn star, the Mn II line at 4136.92 Å should be strong whereas it should be absent in any comparison normal late B-type star. Furthermore, the lines of Mn II at 4206.37 Å and 4252.96 Å should also be enhanced in the spectra of HgMn stars (Gray & Corbally 2009). These three Mn II lines correspond to moderately strong features in HD 67044, they usually are broad lines absorbing 5% of the local continuum. Several other strong Mn II lines could be found and have been used to derive the abundance of manganese.

We find that the strongest expected lines of Ti II, Cr II, Mn II Sr II, Y II, Zr II, Ba II are all indeed strong features in the spectrum of HD 67044. In Table 3, we give a list of the strongest unblended lines of these species together with abundance determinations.

The presence of the Hg II 3983.93 Å line and of several strong Mn II and Sr II, Y II and Zr II lines led us to conclude that HD 67044 is actually another new HgMn star and should be reclassified as such. The abundance determinations presented in next paragraph do confirm this proposal.

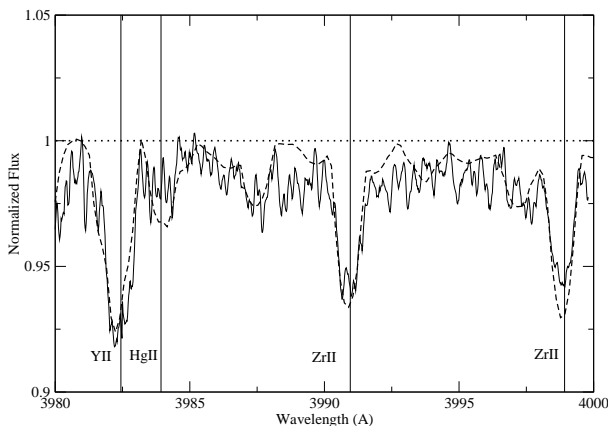


Fig. 1 Comparison of the observed Y II line at 3991.13 Å , Hg II at 3983.93 Å and Zr II line at 3998.96 Å of HD 67044 to a synthetic profile computed for overabundances of 1125 , 200 and 5000 times solar for yttrium, zirconium and mercury respectively.

Table 1 Observation log

Star ID	Spectral type	V	Observation Date	Exposure time (s)	S/N
HD 67044	B 8	7.48	2014-12-16	2400	130
HD 42035	B9V	6.55	2014-12-18	750	174

4 The line spectrum of HD 42035

The high resolution spectrum of HD 42035 is characterised by very sharp lines originating in HD 42035 S. A first estimate of the projected equatorial rotational velocity of HD 42035 S has been obtained by Fourier transform analysis (Fig. 2), using the two Fe II lines at 4508.29 and 4515.34 Å. From the position of the first zero of the Fourier transform, we derived a value of $v_e \sin i = 3.7 \pm 0.2 \text{ km s}^{-1}$. A close inspection of the spectral region around the Mg II triplet at 4481 Å reveals that the spectrum of HD 42035 is actually a composite spectrum containing shallow and broad lines coming from HD 42035 B onto which are overimposed redshifted very sharp lines coming from HD 42035 S. In the SOPHIE spectrum of HD 42035 obtained in December 2014, the sharp lines of the Mg II triplet are displaced, after correction for the barycentric velocity of the Earth, by about $+53.0 \text{ km s}^{-1}$ with respect to their laboratory positions. A comparison in figure 3 of our SOPHIE spectrum of HD 42035 with an archival ELODIE spectrum ($R=42000$) obtained in December 2000 (also corrected for barycentric velocity of the Earth) reveals large radial velocity variations of the sharp lines of the Mg II triplet and possibly a change of the asymmetry of the broad and shallow Mg II line formed in HD 42035 B. Indeed the shallow line had an extended blue wing in December 2014 whereas it had an extended red wing in December 2000. Recent spectroscopy obtained at DAO by E. Griffin confirms large radial velocity variations of the sharp lines and support the binary nature of this star. The composite nature of the spectrum is seen in many features, we show in figure 4 the region of Multiplet 7 of O I.

We have measured the centroids of all sharp lines of HD 42035 S absorbing more than 2 % of the normalized flux by adjusting gaussians. This yields wavelengths accurate to $\pm 0.02 \text{ Å}$. Seven hundred and thirteen line centers were thus measured. In order to identify these lines, a model atmosphere was computed using ATLAS9 (Kurucz 1992) with 72 layers for the effective temperature and surface gravity of HD 42035 (see par. 5.1) and a solar composition. A synthetic spectrum was then computed using SYNSPEC48 (Hubeny & Lanz, 1992) over the entire range 3900 Å to 6800 Å for solar abundances and a microturbulent velocity 0.0 km s^{-1} . It was further convolved with the ROTIN3 routine (provided with SYNSPEC48) for the FWHM of SOPHIE and the $v_e \sin i$ of HD 42035 S. We found that the following species are definitely present in HD 42035 S: He I, C I, C II, Mg II, N I, O I, Na I, Mg I, Mg II, Al I, Al II, Si I, Si II, S II, Ca I, Ca II, Sc I, Sc II, Ti II, V II, Cr I, Cr II, Mn II, Fe I, Fe II, Co II, Sr II and Ba II

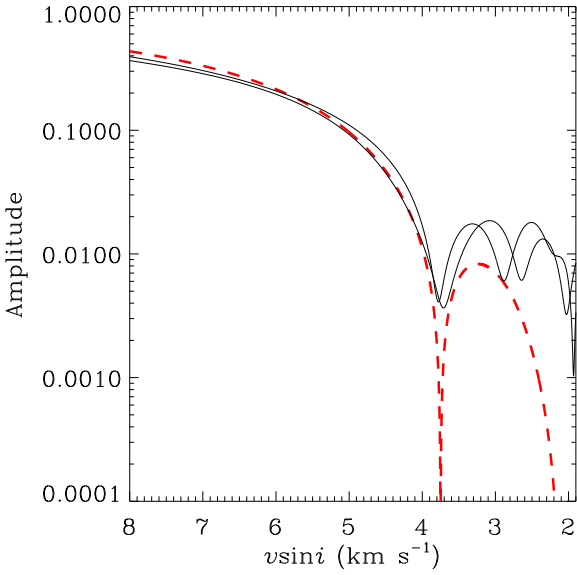


Fig. 2 Fourier transforms of the Fe II lines at 4508.29 and 4515.34 Å (solid lines) and of a synthetic profile with $v_e \sin i = 3.7$ km s $^{-1}$ at a spectral resolution of 75000. On the velocity displayed on the x-axis, the position of the first zero yields the projected equatorial rotational velocity.

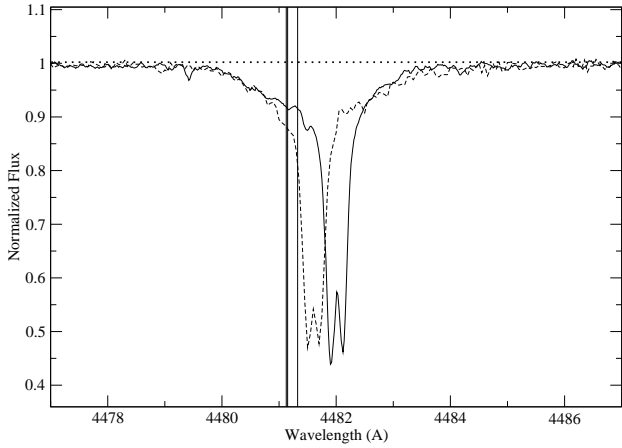


Fig. 3 Comparison of the composite Mg II triplet profile of HD 42035 taken 14 years apart: SOPHIE spectrum (solid line) and archival ELODIE spectrum (dashed line). The vertical lines depict the laboratory wavelengths of the Mg II triplet.

(see Table 5). In contrast, the following elements have very few lines identified and therefore their presence is not confirmed: P II (only one line) and Nd II (only one line). We note the absence of Y II lines and that of lines of Hg II and Pt II characteristic of HgMn stars. Also the lines of Zr II are weak and we could only use one

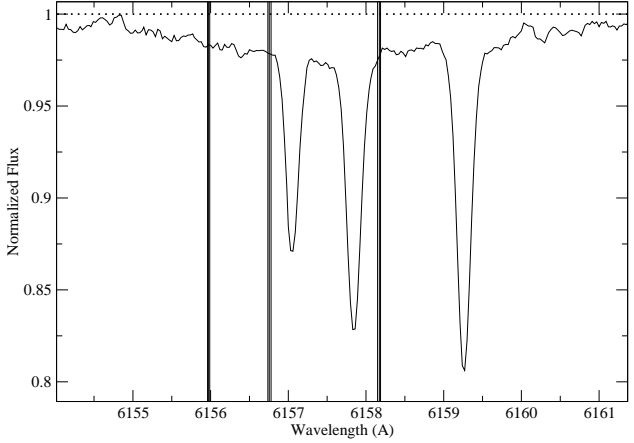


Fig. 4 Composite profile of Multiplet 7 of O I for HD 42035. The vertical lines depict the laboratory wavelengths of the O I lines.

unblended line, $\lambda 4443.008$ Å to derive the zirconium abundance. A few sharp lines have triangular profiles, they all can be identified as Fe II lines

In table 5, we have indicated as “broad” and sometimes “asymmetric” the lines which show a broad shallow component originating in HD 42035 B which can sometimes show an assymetry. These broad and shallow lines are due to N I, O I, Mg II, Si II, Ti II and Fe II. From these identifications, we can infer that HD 42035 B probably has an effective temperature which cannot differ much from that of HD 42035 S.A rough estimate of its projected rotational equatorial velocity has been obtained by adjusting the broad component of the composite Mg II triplet profile at 4481 Å with a model of effective temperature 10740 K, $\log g = 3.80$, solar metallicity and yields $v_e \sin i$ about 150 ± 25 km s $^{-1}$.

5 Abundance determinations

5.1 Fundamental parameters determinations

For HD 67044, we have adopted the effective temperature $T_{\text{eff}} = 10519$ K and surface gravity $\log g = 3.72$ derived by Huang et al. (2010) from fitting the H γ profiles to prediction of model atmospheres. Indeed HD 67044 does not have Strömgren’s photometry which precludes applying Napiwotzky’s (1993) UVBYBETA procedure to derive its fundamental parameters. A spectrum synthesis of the H γ profile was run to confirm these parameters. For HD 42035, the effective temperature, $T_{\text{eff}} = 10740$ K, and surface gravity, $\log g = 3.80$, were also taken from Huang et al. (2010). Applying Napiwotzky’s procedure to the Strömgren’s photometry of

HD 42035 yields very similar fundamental parameters. The effective temperature obtained in this manner is probably a complex mean of the individual effective temperatures of HD 42035 S and HD 42035 B as the Strömgren's photometry most likely measured the combination of the lights of both stars. The adopted effective temperatures, surface gravities, projected equatorial velocities and radial velocities of HD 67044 and HD 42035 S are collected in Table 2.

5.2 Model atmospheres and spectrum synthesis calculations

Plane parallel model atmospheres assuming radiative equilibrium and hydrostatic equilibrium were computed using the ATLAS9 code (Kurucz 1992). The linelist was built from Kurucz (1992) gfhyperall.dat and its revision gfall18sep15.dat² which includes hyperfine splitting levels. A grid of synthetic spectra was computed with SYNSPEC48 (Hubeny & Lanz 1992) to model the lines of He I, C II, O I, Mg II, Al I and Al II, Si II, Ca II, Sc II, Ti II, Cr II, Mn II, Fe II, Sr II, Y II, Zr II, Ba II and Hg II lines. Computations were iterated varying the unknown abundance until minimization of the chi-square between the observed and synthetic spectrum was achieved. The microturbulent velocity was first assumed to be 1.5 km s^{-1} (in agreement with the run of v_{micr} with T_{eff} we established in Gebran et al. (2014)). The synthesis of the Fe II lines of various strengths however imposed a lower $v_{micr} = 0 \text{ km s}^{-1}$ for HD 67044 typical of an HgMn star. A null microturbulent velocity was also finally adopted for HD 42035 S after unsuccessful attempts to model the Fe II lines with higher velocities.

5.3 The derived abundances of HD 67044

We have used only unblended lines to derive the abundances. There are actually few unblended lines as the projected equatorial velocity of HD 67044 broadens significantly the lines. For a given element, the final abundance is a weighted mean of the abundances derived for each transition. These final abundances and their estimated uncertainties for HD 67044 are collected in Table

²<http://kurucz.harvard.edu/linelists/gfnew/gfall28sep15.dat>

Table 2 Fundamental parameters

Star ID	T_{eff}	$\log g$	$v \sin i$ (km s^{-1})	V_{rad} (km s^{-1})
HD 67044	10519	3.72	45.0	14.50
HD 42035 S	10740	3.80	3.7	53.00

3 (the determination of the uncertainties is discussed in Royer et al. 2014). Table 3 contains for each analysed species the adopted laboratory wavelength, logarithm of oscillator strength, its source, the logarithm of the absolute abundance normalised to that of hydrogen (on a scale where $\log(N_H) = 12$) for each transition, and the final abundance and estimated uncertainty. In this work, we adopted Asplund et al. (2009) abundances for the Sun as a reference.

The iron abundance, which is found to be about solar in HD 67044, has been derived mostly by using several Fe II lines of multiplets 37, 38 and 186 in the range 4500–4600 Å whose atomic parameters are critically assessed in NIST³ (these are C+ and D quality lines). These lines are widely spaced and the continuum is fairly easy to trace in this spectral region. Their synthesis always yields consistent iron abundances from the various transitions with very little dispersion. The iron abundance is probably the most accurately determined of the abundances derived here. The NLTE abundance correction for the $\lambda 4471.48 \text{ \AA}$ He I line is very small as shown by Lemke (1989) for early A-type stars and we have not corrected for it. We find that the following species are underabundant: He, C, O, Si, Ca, Sc while Mg, V, Fe and Ni show mild enhancements (less than 5 times solar) and Ti, Cr, Mn, Sr, Y, Zr, Ba and Hg show pronounced overabundances (larger than 5 times solar), the largest overabundance being for Hg. The Sr-Y-Zr triad is inverted, yttrium being more abundant than strontium and zirconium. The general trend is that the heaviest elements are the most overabundant.

5.4 The provisional abundances for HD 42035 S

Assuming an effective temperature of 10740 K, $\log g = 3.80$ and a solar composition, for HD 42035 S, we have derived provisional abundances for HD 42035 S which are collected in Table 4. The effective temperature of HD 42035 S is probably different from this mean value so that the derived abundances are rough estimates only. Furthermore, placing a continuum level in the composite spectrum of HD 42035 turned out to be difficult because of the presence of the rotationally broadened lines and of the continuum of HD 42035 B. The provisional abundances we derive here are therefore affected by systematic errors due to (at least) the possibility of an improper placement of the continuum (too low compared to what it actually is). As a consequence, the residual fluxes $\frac{F}{F_c}$ are likely to be too large, placing the continuum higher would decrease these residual fluxes

³<http://www.nist.gov>

and therefore lead to higher abundances. We therefore consider that the provisional abundances derived here are lower limits. The actual abundances of HD 42035 S must be larger than these lower limits. To minimize this effect we chose to synthesize sharp lines which were as little as possible blended with the broad lines of HD 42035 B. Realistic abundances will only be derived if we manage to disentangle the spectrum of HD 42035 S from that of HD 42035 B.

We find that the light elements up to Z=21, C, O, Mg, Al, Si, S, Ca and Sc are all underabundant. The scandium deficiency is large (about 4 % of the solar scandium abundance). The elements heavier than Z=21 are overabundant except for Ti, Fe and Sr which are underabundant. The zirconium overabundance has been derived from only one unblended line and thus should be taken with caution. The absence of detection of the two strongest Y II lines at 3982.60 Å and 5662.92 Å implies that yttrium must be solar or underabundant.

of the actual abundances of HD 42035 S because we are probably placing the continuum too low. A complete follow-up of this new spectroscopic binary will hopefully enable a proper disentangling of the spectra of HD 42035 S and HD 42035 B and help characterize fully the nature of each of these components, in particular the nature and abundance pattern of HD 42035 S.

We thank the referee, Dr. Fiorella Castelli, for her insightful comments which resulted into many improvements. We also thank the OHP night assistants for their helpful support during the three observing runs. We acknowledge the use of the ELODIE archive at OHP.

6 Conclusions

We find that HD 67044, hitherto classified a normal B8 star, displays underabundances of He, C, O, Si, Ca and Sc, mild overabundances of Mg, V, Fe and Ni and pronounced enhancements of Ti, Cr, Mn, Sr, Y, Zr, Ba and Hg.. We therefore propose that HD 67044 actually is a new HgMn star and should be reclassified as such. Current monitoring of HD 67044 suggests that the Hg II line at 3983.93 Å is probably variable. One possible interpretation is that HD 67044 has one or several spots of overabundant Hg over its surface. More observations are planned to address this issue.

The high resolution spectrum of HD 42035 appears to be a composite spectrum where redshifted very sharp lines originating from HD 42035 S are overimposed onto the broad shallow lines originating from HD 42035 B. The presence of a very slow rotator and a fairly fast rotator inside the same system suggests that the semi-axis of the orbit must be large. A FT analysis of the sharp lines of HD 42035 S yields a very low projected equatorial velocity ($v_e \sin i = 3.7 \text{ km s}^{-1}$) which makes this star one of the very few late-B type slow rotators. The identification of 713 very sharp lines reveals that most of the lines are due to elements up to Nickel. Strontium and Barium are also present. Assuming a similar effective temperature and surface gravity for HD 42035 S and HD 42035 B, we have derived provisional abundances for HD 42035 S. Light elements up to Z=22 appear to be underabundant in HD 42035 S whereas heavier elements are overabundant with the exception of Fe and Sr. These preliminary abundances are lower limits

References

- Asplund, M., Grevesse, N., Sauval, A. J., & Scott, P. 2009, Annu. Rev. Astron. Astrophys., 47, 481
- Biémont, É., Blagoev, K., Engström, L., et al. 2011, Mon. Not. R. Astron. Soc., 414, 3350
- Biemont, E., Grevesse, N., Hannaford, P., & Lowe, R. M. 1981, *Astrophys. J.*, 248, 867
- Biermann, L. & Lübeck, K. 1948, *Z. Astrophys.*, 25, 325
- Butler, K. & Zeippen, C. J. 1991, *J. Phys. IV France*, 01, C1
- Cowley, A. 1972, *Astron. J.*, 77, 750
- Davidson, M. D., Snoek, L. C., Volten, H., & Doenszelmann, A. 1992, *Astron. Astrophys.*, 255, 457
- Dolk, L., Wahlgren, G. M., & Hubrig, S. 2003, *Astron. Astrophys.*, 402, 299
- Drake, G. 2006, Springer Handbook of Atomic, Molecular, and Optical Physics, ed. G. Drake (New York, NY: Springer New York), 199–219
- Fuhr, J. R., Martin, G. A., & Wiese, W. L. 1988, Journal of Physical and Chemical Reference Data, 17
- Gebran, M., Monier, R., Royer, F., Lobel, A., & Blomme, R. 2014, in Putting A Stars into Context: Evolution, Environment, and Related Stars, ed. G. Mathys, E. R. Griffin, O. Kochukhov, R. Monier, & G. M. Wahlgren, 193–198
- Gray, R. O. & Corbally, J., C. 2009, Stellar Spectral Classification
- Hannaford, P. 1999, *Microchemical Journal*, 63, 43
- Hibbert, A., Biémont, E., Godefroid, M., & Vaeck, N. 1991, *Journal of Physics B: Atomic, Molecular and Optical Physics*, 24, 3943
- Huang, W., Gies, D. R., & McSwain, M. V. 2010, *Astrophys. J.*, 722, 605
- Hubeny, I. & Lanz, T. 1992, *Astron. Astrophys.*, 262, 501
- Kaufman, V. & Hagan, L. 1979, *J. Opt. Soc. Am.*, 69, 232
- Kling, R., Schnabel, R., & Griesmann, U. 2001, *The Astrophysical Journal Supplement Series*, 134, 173
- Kostyk, R. I. & Orlova, T. V. 1983, *Astrometriia i Astrofizika*, 49, 39
- Kurucz, R. L. 1992, *Rev. Mexicana Astron. Astrofis.*, 23
- Lawler, J. E. & Dakin, J. T. 1989, *J. Opt. Soc. Am. B*, 6, 1457
- Lemke, M. 1989, *Astron. Astrophys.*, 225, 125
- Ljung, G., Nilsson, H., Asplund, M., & Johansson, S. 2006, *Astron. Astrophys.*, 456, 1181
- Martin, W. C. 1960, *J. Opt. Soc. Am.*, 50, 174
- Matheron, P., Escarguel, A., Redon, R., Lesage, A., & Richou, J. 2001, *Journal of Quantitative Spectroscopy and Radiative Transfer*, 69, 535
- Meggers, W. F., Corliss, C. H., & Scribner, B. F. 1975, Tables of spectral-line intensities. Part I, II - arranged by elements.
- Miles, B. M. & Wiese, W. L. 1969, *Atomic Data*, 1, 1
- Monier, R., Gebran, M., & Royer, F. 2015, *Astron. Astrophys.*, 577, A96
- Napiwotzki, R., Schoenberner, D., & Wenske, V. 1993, *Astron. Astrophys.*, 268, 653
- Nave, G. & Johansson, S. 2013, *The Astrophysical Journal Supplement Series*, 204, 1
- Nussbaumer, H. & Storey, P. J. 1981, *Astron. Astrophys.*, 96, 91
- Palacios, A., Gebran, M., Josselin, E., et al. 2010, *Astron. Astrophys.*, 516, A13
- Perruchot, S., Kohler, D., Bouchy, F., et al. 2008, in Proc. SPIE, Vol. 7014, Ground-based and Airborne Instrumentation for Astronomy II, 70140J
- Pickering, J. C., Thorne, A. P., & Perez, R. 2002, *Astrophys. J. Suppl. Ser.*, 138, 247
- Pinnington, E. H., Berends, R. W., & Lumsden, M. 1995, *Journal of Physics B: Atomic, Molecular and Optical Physics*, 28, 2095
- Raassen, A. J. J. & Uylings, P. H. M. 1998, *Journal of Physics B Atomic Molecular Physics*, 31, 3137
- Royer, F., Gebran, M., Monier, R., et al. 2014, *Astron. Astrophys.*, 562, A84
- Sansonetti, C. J. & Nave, G. 2014, *The Astrophysical Journal Supplement Series*, 213, 28
- Sansonetti, C. J. & Reader, J. 2001, *Physica Scripta*, 63, 219
- Shenstone, A. G. 1961, *Proceedings of the Royal Society of London A: Mathematical, Physical and Engineering Sciences*, 261, 153
- Siegel, W., Migdalek, J., & Kim, Y.-K. 1998, *Atomic Data and Nuclear Data Tables*, 68, 303
- Theodosiou, C. E. 1989, *Phys. Rev. A*, 39, 4880
- Wiese, W. L., Fuhr, J. R., & Deters, T. M. 1996, Atomic transition probabilities of carbon, nitrogen, and oxygen : a critical data compilation

Table 3 Elemental Abundances for HD67044. References are MA60 for Martin (1960), DR2006 for Drake (2006), NS81 for Nussbaumer & Storey (1981), KZ91 for Butler, K. & Zeippen, C. J. (1991), W96 for Wiese et al. (1996), HBGV91 for Hibbert et al. (1991), Si98 for Siegel et al. (1998), K79 for Kaufman & Hagan (1979), H99 for Hannaford (1999), Ma01 for Matheron et al. (2001), Sh61 for Shenstone (1961), LD89 for Lawler & Dakin (1989), FMW for Fuhr et al. (1988), PTP for Pickering et al. (2002), SN14 for Sansonetti & Nave (2014), NJ13 for Nave & Johansson (2013), T89 for Theodosiou (1989), RU98 for Raassen & Uylings (1998), PBL95 for Pinnington et al. (1995), NBS for Miles & Wiese (1969), KO83 for Kostyk & Orlova (1983), Bie11 for Biémont et al. (2011), L06 for Ljung et al. (2006), MCS75 for Meggers et al. (1975), BL48 for Biermann & Lübeck (1948), Bal81 for Biemont et al. (1981), KL01 for Kling et al. (2001), DSVD92 for Davidson et al. (1992), SR01 for Sansonetti & Reader (2001), Do03 for Dolk et al. (2003), NIST for the online database (<http://physics.nist.gov/PhysRefData/ASD/>), and Kurucz (<http://kurucz.harvard.edu/linelists/gfhyperall/>) for the gfhyperall.dat linelist.

Element	λ (Å)	$\log gf$	Ref.	$\log(X/H)_\star$
He I	4471.470	-2.211	Ma60/DR2006	-1.17
He I	4471.474	-0.287	Ma60/DR2006	-1.17
He I	4471.474	-1.035	Ma60/DR2006	-1.17
He I	4471.485	-1.035	Ma60/DR2006	-1.17
He I	4471.489	-0.558	Ma60/DR2006	-1.17
He I	4471.683	-0.910	Ma60/DR2006	-1.17
He I	5875.598	-1.516	Ma60/DR2006	-1.13
He I	5875.613	-0.339	Ma60/DR2006	-1.13
He I	5875.615	0.409	Ma60/DR2006	-1.13
He I	5875.625	-0.339	Ma60/DR2006	-1.13
He I	5875.640	0.138	Ma60/DR2006	-1.13
He I	5875.966	-0.214	Ma60/DR2006	-1.15
$[\frac{He}{H}] = -0.15 \pm 0.15 \text{ dex}$				
C II	4267.001	0.563	NS81	-4.06
C II	4267.261	0.716	NS81	-4.10
C II	4267.261	-0.584	NS81	-4.10
$[\frac{C}{H}] = -0.60 \pm 0.15 \text{ dex}$				
O I	5329.673	-2.063	KZ91/W96	-3.39
O I	5330.726	-2.416	KZ91/W96	-3.37
O I	5330.741	-0.983	KZ91/W96	-3.37
O I	6155.961	-1.363	HBGV91	-3.41
O I	6155.971	-1.011	HBGV91	-3.41
O I	6155.989	-1.120	HBGV91	-3.41
O I	6156.737	-1.487	HBGV91	-3.37
O I	6155.755	-0.898	HBGV91	-3.37
O I	6156.778	-0.694	HBGV91	-3.37
O I	6158.149	-1.841	HBGV91	-3.39
O I	6158.172	-0.995	HBGV91	-3.39
O I	6158.187	-0.409	HBGV91	-3.39
$[\frac{O}{H}] = -0.22 \pm 0.20 \text{ dex}$				
Mg II	4390.572	-0.523	Si98	-4.25
Mg II	4427.994	-1.208	Si98	-4.29
Mg II	4481.126	0.749	BL48	-4.27
Mg II	4481.150	-0.553	BL48	-4.27
Mg II	4481.325	0.594	BL48	-4.27
$[\frac{Mg}{H}] = 0.15 \pm 0.18 \text{ dex}$				
Al II	4663.056	-0.244	K79	-5.56
Al I	3944.006	-0.635	H99	-5.60

Table 3—Continued

Element	λ (Å)	$\log g f$	Ref.	$\log(X/H)_*$
$[\frac{Al}{H}] = -0.04 \pm 0.20$ dex				
Si II	4128.054	0.359	Ma01	-4.52
Si II	4130.894	0.552	Ma01	-4.56
Si II	4190.72	-0.351	Sh61	-4.54
Si II	5041.024	0.029	Ma01	-4.56
Si II	5055.984	0.523	Ma01	-4.54
Si II	5056.317	-0.492	Ma01	-4.52
Si II	6347.11	0.149	Ma01	-4.54
Si II	6371.37	-0.082	Ma01	-4.56
$[\frac{Si}{H}] = -0.086 \pm 0.18$ dex				
Ca II	3933.663	0.135	NIST/T89	-6.02
Ca II	5019.971	-0.28	NIST/T89	-6.06
$[\frac{Ca}{H}] = -0.40 \pm 0.20$ dex				
Sc II	4246.822	0.242	LD89	-9.05
Sc II	4670.407	-0.580	LD89	-9.09
Sc II	5031.021	-0.400	LD89	-9.07
Sc II	5526.813	-0.77	LD89	-9.07
$[\frac{Sc}{H}] = -0.24 \pm 0.18$ dex				
Ti II	4163.644	-0.128	PTP	-5.97
Ti II	4287.873	-2.020	PTP	-6.01
Ti II	4290.210	-0.848	PTP	-5.99
Ti II	4294.090	-1.100	PTP	-5.96
Ti II	4300.042	-0.442	PTP	-5.97
Ti II	4411.072	-0.6767	PTP	-6.01
Ti II	4468.492	-0.620	FMW	-5.99
Ti II	4549.622	-0.105	PTP	-5.97
Ti II	4563.758	-0.96	Kurucz	-5.99
Ti II	5129.156	-1.239	KO83	-5.97
Ti II	5188.687	-1.220	PTP	-6.00
Ti II	5336.780	-1.700	PTP	-6.01
$[\frac{Ti}{H}] = 0.99 \pm 0.20$ dex				
Cr II	4558.644	-0.660	SN14	-5.39
Cr II	4558.787	-2.460	SN14	-5.39
Cr II	5237.322	-1.160	SN14	-5.43
Cr II	5308.421	-1.810	SN14	-5.39
Cr II	5313.581	-1.650	SN14	-5.41
Cr II	5502.086	-1.990	SN14	-5.43
$[\frac{Cr}{H}] = 0.92 \pm 0.18$ dex				
Mn II	4206.368	-1.54	KL01	-5.59
Mn II	4259.19	-1.44	KL01	-5.63
$[\frac{Mn}{H}] = 1.060 \pm 0.20$ dex				
Fe II	4233.162	-1.810	NJ13	-4.34
Fe II	4258.148	-3.500	NJ13	-4.30
Fe II	4273.326	-3.350	NJ13	-4.32
Fe II	4296.566	-2.900	NJ13	-4.30

Table 3—Continued

Element	λ (Å)	$\log gf$	Ref.	$\log(X/H)_\star$
Fe II	4491.397	-2.640	NJ13	-4.34
Fe II	4508.280	-2.300	NJ13	-4.32
Fe II	4515.333	-2.360	NJ13/RU98	-4.34
Fe II	4520.218	-2.600	NJ13/RU98	-4.32
Fe II	4522.628	-1.990	NJ13/RU98	-4.34
Fe II	4549.195	-1.770	NJ13/RU98	-4.30
Fe II	4549.466	-1.730	NJ13/RU98	-4.30
Fe II	4555.888	-2.250	NJ13/RU98	-4.32
Fe II	4923.921	-1.210	NJ13	-4.34
Fe II	5275.997	-1.900	NJ13	-4.30
Fe II	5316.609	-1.780	NJ13/RU98	-4.32
Fe II	5506.199	0.860	NJ13	-4.30
$[\frac{Fe}{H}] = 0.18 \pm 0.18$ dex				
Sr II	4215.519	-0.173	PBL95	-7.67
$[\frac{Sr}{H}] = 1.40 \pm 0.25$ dex				
Y II	3982.592	-0.560	Bie11	-6.71
Y II	5662.922	0.340	Bie11	-6.75
$[\frac{Y}{H}] = 3.05 \pm 0.25$ dex				
Zr II	3991.127	-0.310	L06	-7.11
Zr II	3998.965	-0.520	L06	-7.09
Zr II	4442.992	-0.420	L06	-7.07
Zr II	4457.431	-1.220	L06	-7.09
Zr II	4496.962	-0.890	L06	-7.07
Zr II	5112.270	-0.850	L06	-7.11
$[\frac{Zr}{H}] = 2.30 \pm 0.25$ dex				
Ba II	4934.077	-0.156	NBS	-7.63
Ba II	6141.713	-0.032	DSVD92	-7.59
$[\frac{Ba}{H}] = 2.18 \pm 0.25$ dex				
Hg II	3983.931	-1.510	SR01/Do03	-7.21
$[\frac{Hg}{H}] = 3.70 \pm 0.25$ dex				

Table 4 Provisional Elemental Abundances for HD42035 S

Element	λ (Å)	$\log g f$	Ref.	$\log(X/H)_\star$
C II	4267.001	0.563	NS81	-3.63
C II	4267.261	0.716	NS81	-3.63
C II	4267.261	-0.584	NIST	-3.63
$[\frac{C}{H}] = -0.15 \pm 0.15 \text{ dex}$				
O I	6155.961	-1.363	HBGV91	-3.47
O I	6155.971	-1.011	HBGV91	-3.47
O I	6155.989	-1.120	HBGV91	-3.47
O I	6156.737	-1.487	HBGV91	-3.47
O I	6155.755	-0.898	HBGV91	-3.47
O I	6156.778	-0.694	HBGV91	-3.47
O I	6158.149	-1.841	HBGV91	-3.47
O I	6158.172	-0.995	HBGV91	-3.47
O I	6158.187	-0.409	HBGV91	-3.47
$[\frac{O}{H}] = -0.30 \pm 0.20 \text{ dex}$				
Mg II	4390.572	-0.530	Si98	-4.94
Mg II	4427.994	-1.201	Si98	-4.94
Mg II	4481.126	0.730	BL48	-4.94
Mg II	4481.150	-0.570	BL48	-4.94
Mg II	4481.325	0.575	BL48	-4.94
$[\frac{Mg}{H}] = -0.52 \pm 0.18 \text{ dex}$				
Al II	5593.27	+0.41	K79	-5.83
Al II	6243.40	+0.67	K79	-5.83
$[\frac{Al}{H}] = -0.30 \pm 0.20 \text{ dex}$				
Si II	4128.054	0.306	Ma01	-5.05
Si II	4130.88	0.464	Ma01	-5.05
Si II	4190.72	-0.351	Sh61	-4.85
Si II	5041.024	0.174	Ma01	-4.80
Si II	5055.984	0.441	Ma01	-4.85
Si II	5056.317	-0.535	Ma01	-4.75
Si II	6347.11	0.230	Ma01	-4.85
Si II	6371.37	-0.080	Ma01	-4.85
$[\frac{Si}{H}] = -0.43 \pm 0.18 \text{ dex}$				
S II	4162.665	0.830	Kurucz	-4.97
$[\frac{S}{H}] = -0.30 \pm 0.20 \text{ dex}$				
Ca II	3933.663	-0.135	NIST/T89	-5.94
Ca II	5019.971	-0.257	NIST/T89	-5.94
$[\frac{Ca}{H}] = -0.30 \pm 0.20 \text{ dex}$				
Sc II	4246.86	0.242	LD89	-10.23
Sc II	4314.06	-0.10	LD89	-10.23
Sc II	4400.38	-0.51	LD89	-10.23
Sc II	5031.021	-0.400	LD89	-10.23
$[\frac{Sc}{H}] = -1.40 \pm 0.18 \text{ dex}$				
Ti II	4163.644	-0.130	PTP	-7.20
Ti II	4287.873	-1.790	PTP	-7.20
Ti II	4290.210	-0.850	PTP	-7.28

Table 4—Continued

Element	λ (Å)	$\log gf$	Ref.	$\log(X/H)_*$
Ti II	4300.042	-0.440	PTP	-7.20
Ti II	4411.072	-0.670	PTP	-6.98
Ti II	4549.62	-0.470	PTP	-7.20
Ti II	4563.77	-0.96	Kurucz	-7.20
Ti II	5129.156	-1.400	KO83	-7.20
Ti II	5188.687	-1.050	PTP	-7.28
$[\frac{T_i}{H}] = -0.21 \pm 0.20$ dex				
V II	4005.706	-0.460	Kurucz	-7.30
V II	4023.360	-0.880	Kurucz	-7.30
V II	4035.610	-0.960	Kurucz	-7.30
$[\frac{V}{H}] = 0.70 \pm 0.20$ dex				
Cr II	4558.650	-0.660	SN14	-5.93
Cr II	4558.78	-2.460	SN14	-5.93
Cr II	5237.329	-1.160	SN14	-6.02
Cr II	5308.440	-1.810	SN14	-6.02
Cr II	5502.067	-1.990	SN14	-6.02
$[\frac{Cr}{H}] = 0.35 \pm 0.18$ dex				
Mn II	4206.368	-1.566	KL01	-5.77
Mn II	4259.19	-1.589	KL01	-5.77
$[\frac{Mn}{H}] = 0.85 \pm 0.20$ dex				
Fe II	4233.172	-2.000	NJ13	-5.50
Fe II	4258.154	-3.400	NJ13	-4.90
Fe II	4273.326	-3.258	NJ13	-4.80
Fe II	4296.570	-3.010	NJ13	-4.90
Fe II	4491.405	-2.690	NJ13	-5.32
Fe II	4508.281	-2.210	NJ13	-5.32
Fe II	4515.334	-2.490	NJ13/RU98	-5.20
Fe II	4520.221	-2.600	NJ13/RU98	-5.20
Fe II	4522.628	-2.030	NJ13/RU98	-5.50
Fe II	4549.197	-1.870	NJ13/RU98	-4.50
Fe II	4549.467	-1.750	NJ13/RU98	-5.50
Fe II	4555.888	-2.290	NJ13/RU98	-5.20
Fe II	4923.927	-1.320	NJ13	-5.32
Fe II	5276.002	-1.940	NJ13	-5.20
Fe II	5316.615	-1.850	NJ13/RU98	-5.20
Fe II	5506.195	0.950	NJ13	-5.02
$[\frac{Fe}{H}] = -0.66 \pm 0.18$ dex				
Ni II	5058.38	+0.85	Kurucz	-4.75
Ni II	5059.17	+0.54	Kurucz	-4.75
$[\frac{Ni}{H}] = 1.00 \pm 0.25$ dex				
Sr II	4077.709	0.148	PBL95	-9.53
Sr II	4215.520	-0.173	PBL95	-9.53
$[\frac{Sr}{H}] = -0.46 \pm 0.25$ dex				
Y II	5662.93	0.16	MCS75	-9.78
$[\frac{Y}{H}] = 0.00 \pm 0.25$ dex				

Table 4—Continued

Element	λ (Å)	$\log gf$	Ref.	$\log(X/H)_\star$
Zr II	4443.008	-0.330	L06	-8.69
	$[\frac{Zr}{H}] = 0.70 \pm 0.25$ dex			
Ba II	4554.029	+0.170	NBS	-9.31
Ba II	4934.076	-0.156	NBS	-9.31
Ba II	6496.897	-0.380	DSVD92	-9.31
	$[\frac{Ba}{H}] = 0.48 \pm 0.25$ dex			

Table 5 Proposed line identifications for HD 42035 S

Corr. λ (Å)	Lab. λ (Å)	Ident.	E_{low} (cm $^{-1}$)	$\log(gf)$	Rem.
3900.54	3900.550	Ti II	9118.260	-0.45	
3902.95	3902.945	Fe I	12560.933	-0.47	
3903.26	3903.268	V II	11908.270	-0.89	
3903.74	3903.756	Fe II	60807.228	-1.49	
3905.52	3905.525	Si I	15394.369	-1.09	
3905.64	3905.644	Cr II	42986.619	-0.90	
3906.03	3906.035	Fe II	44929.549	-1.83	
3913.46	3913.468	Ti II	8997.710	-0.53	
3914.50	3914.503	Fe II	13474.411	-4.05	
3918.52	3918.528	Fe II	47674.718	-2.10	
3918.95	3918.965	C II	131724.372	-0.51	
3920.63	3920.635	Fe II	60625.451	-1.20	
3921.99	3922.004	Fe II	72603.502	-1.06	
3922.90	3922.908	Mg I	35051.263	-3.53	
3927.92	3927.920	Fe I	888.132	-1.59	
3930.30	3930.297	Fe I	704.007	-1.59	
	3930.304	Fe II	13673.186	-4.03	
3932.00	3932.023	Ti II	9118.260	-1.78	
3933.23	3933.245	Fe II	78690.849	-3.39	
3933.34	3933.345	V II	47101.889	-2.69	
3933.66	3933.663	Ca II	0.000	0.13	
3935.95	3935.962	Fe II	44915.046	-1.86	
3938.29	3938.290	Fe II	13474.411	-3.89	
3938.97	3938.970	Fe II	47674.718	-1.85	
3944.00	3944.006	Al I	0.000	-0.62	
3945.20	3945.210	Fe II	13673.186	-4.25	
3947.29	3947.295	O I	73768.202	-2.28	
3947.48	3947.481	O I	73768.202	-2.43	
3951.94	3951.930	Ni II	94705.927	-2.78	
	3951.965	V II	11908.270	-0.74	
3960.89	3960.899	Fe II	58631.532	-1.42	
3961.51	3961.520	Al I	112.061	-0.32	
3968.46	3968.469	Ca II	0.000	-0.17	
3979.51	3979.505	Cr II	45730.581	-0.73	
4002.08	4002.083	Fe II	22409.852	-3.47	
4002.53	4002.543	Fe II	48039.087	-1.71	
4002.93	4002.936	V II	11514.760	-1.81	
4003.28	4003.283	Cr II	52297.808	-0.60	
4005.24	4005.242	Fe I	12560.933	-0.61	
4005.70	4005.706	V II	14655.630	-0.46	
4012.50	4012.496	Cr II	45669.369	-0.89	
4015.47	4015.474	Ni II	32523.540	-2.42	
4023.36	4023.388	V II	14556.090	-0.88	
4024.54	4024.547	Fe II	36252.917	-2.48	

Table 5—Continued

Corr. λ (Å)	Lab. λ (Å)	Ident.	E_{low} (cm $^{-1}$)	$\log(gf)$	Rem.
4025.12	4025.131	Ti II	4897.650	-1.98	
4026.26	4026.201	He I	169086.766	-2.629	
4026.26	4026.201	He I	169086.766	-1.453	
4026.26	4026.201	He I	169086.766	-0.705	
4026.26	4026.201	He I	169086.843	-1.453	
4026.26	4026.201	He I	169086.843	-0.976	
4028.33	4028.343	Ti II	15257.430	-1.00	
4028.77	4028.750	S II	128599.162	-0.12	
4030.34	4030.358	Cr II	25033.700	-3.56	
	4030.358	Fe II	88723.398	-0.99	
4030.72	4030.730	Mn I	0.000	-0.47	
4031.45	4031.442	Fe II	38164.195	-3.11	
4032.94	4032.935	Fe II	36252.917	-2.70	
4035.61	4035.627	V II	14461.750	-0.96	
4037.95	4037.972	Cr II	52321.010	-0.56	
4044.00	4044.012	Fe II	44929.549	-2.41	
4045.80	4045.812	Fe I	11976.238	0.28	
4048.83	4048.830	Fe II	44915.046	-2.15	
4049.09	4049.097	Cr II	52297.808	-0.86	
4051.93	4051.930	Cr II	25033.700	-2.19	
4053.82	4053.834	Ti II	15265.619	-1.21	
4054.08	4054.076	Cr II	25046.759	-2.47	
4057.46	4057.461	Fe II	58666.256	-1.55	
4061.77	4061.782	Fe II	48039.087	-2.65	
4063.59	4063.594	Fe I	12560.933	0.07	
4067.03	4067.031	Ni II	32499.529	-1.29	
4069.88	4069.883	Fe II	47674.718	-2.75	
4070.64	4070.630	Fe II	60625.451	-3.01	
	4070.632	Fe II	62151.561	-2.98	
4070.83	4070.840	Cr II	52321.010	-0.75	
4071.04	4071.007	Ni II	32523.540	-3.47	
4071.57	4071.564	V I	15572.030	-0.19	
4071.73	4071.738	Fe I	12968.554	-0.02	
4072.08	4072.097	Co II	25147.370	-4.72	
4072.56	4072.561	Cr II	29951.880	-2.41	
4072.70	4072.709	Si II	79338.550	-2.37	
4075.44	4075.452	Si II	79355.019	-1.40	
4075.93	4075.954	Fe II	20516.959	-3.38	
4076.78	4076.780	Si II	79338.502	-1.67	
4077.16	4077.15	Ti I	17423.855	-0.65	
4077.71	4077.709	Sr II	0.000	0.17	
4110.98	4110.990	Cr II	30307.439	-2.02	
	4111.003	Cr II	25033.700	-1.92	
4111.85	4111.877	Fe II	48039.087	-2.16	

Table 5—Continued

Corr. λ (Å)	Lab. λ (Å)	Ident.	E_{low} (cm $^{-1}$)	$\log(gf)$	Rem.
4113.23	4113.212	Cr II	25046.749	-2.27	
4118.54	4118.545	Fe I	28819.952	0.29	
4119.51	4119.524	Fe II	20516.959	-4.92	
4120.85	4120.846	P II	103339.144	-2.87	
4122.66	4122.668	Fe II	20830.582	-3.38	
4124.77	4124.787	Fe II	20516.959	-4.20	
4127.03	4127.057	Cr II	45730.581	-1.77	
4128.06	4128.054	Si II	79338.502	0.32	Mult 2
4128.74	4128.748	Fe II	20830.582	-3.77	
4130.88	4130.872	Si II	79355.019	-0.82	Mult 2
	4130.894	Si II	79355.019	0.48	Mult 2
4132.05	4132.058	Fe II	12968.554	-0.65	
4132.42	4132.419	Cr II	30307.439	-2.35	
4142.23	4142.259	S II	127825.085	0.24	
4143.42	4143.415	Fe I	24574.652	-0.20	
4143.86	4143.868	Fe I	12560.933	-0.45	
4145.07	4145.060	S II	127976.340	0.23	
4145.78	4145.781	Cr II	42897.990	-1.16	
4153.06	4153.068	S II	128233.187	0.39	
4156.82	4156.799	Fe I	22838.320	-0.62	
4160.63	4160.623	Fe II	22939.357	-5.04	
4161.08	4161.075	Cr II	42986.619	-2.470	
4161.52	4161.535	Ti II	8744.250	-2.360	
4162.67	4162.665	S II	128599.162	0.83	
4167.30	4167.299	Fe II	90300.626	-0.56	
4171.88	4171.903	Cr II	25042.811	-2.38	
4173.44	4173.461	Fe II	20850.582	-2.18	
4177.68	4177.692	Fe II	20516.959	-3.75	
4178.84	4178.862	Fe II	20830.582	-2.48	
4179.42	4179.42	Cr II	30864.459	-1.77	
4181.73	4181.732	Cr II	93574.441	-2.38	
4187.03	4187.039	Fe I	19757.031	-0.55	
4187.82	4187.805	V II	32299.271	-1.62	
4190.72	4190.707	Si II	108820.600	0.20	
4191.43	4191.430	Fe I	19912.494	-0.67	
4192.02	4192.065	Ni II	32523.540	-3.06	
4195.38	4195.365	Fe II	61041.746	-3.88	
4196.17	4196.19	Fe II	90042.781	-3.04	
4198.11	4198.134	Si II	108778.702	-0.30	
4198.29	4198.304	Fe I	19350.891	-0.72	
4199.09	4199.093	Fe II	37227.326	-3.99	
	4199.095	Fe I	24574.652	0.25	
4199.48	4199.491	Fe II	89924.175	-0.23	
4200.49	4200.521	Fe II	90067.346	-0.30	

Table 5—Continued

Corr. λ (Å)	Lab. λ (Å)	Ident.	E_{low} (cm $^{-1}$)	$\log(gf)$	Rem.
4200.91	4200.898	Si II	101024.349	-0.67	
4202.02	4202.029	Fe I	11976.238	-0.71	
4202.52	4202.522	Fe II	54902.315	-2.33	
4205.58	4205.595	Fe II	90386.527	-0.30	
4210.35	4210.343	Fe I	20019.633	-0.87	
4215.52	4215.519	Sr II	0.000	-0.14	
4219.36	4219.360	Fe I	28819.952	0.12	
4224.85	4224.860	Cr II	42986.619	-1.73	
4226.72	4226.728	Ca I	0.000	0.24	
4227.42	4227.427	Fe I	26874.547	0.23	
4230.38	4230.375	Ni I	30619.440	-2.12	
4232.47	4232.488	Ca I	39464.809	-2.60	
4232.87	4232.849	Si II	97972.086	-1.00	
4233.17	4233.172	Fe II	20830.582	-2.00	
4233.62	4233.602	Fe I	20019.633	-0.60	
4233.97	4233.977	V I	15688.870	-0.02	
4234.15	4234.167	Nd II ?	1470.105	-0.99	
4235.44	4235.421	Cr II	86782.041	-2.49	
4235.92	4235.936	Fe I	19562.437	-0.34	
4238.81	4238.791	Mn II	14781.190	-3.63	
4242.36	4242.364	Cr II	31219.350	-0.59	
4244.77	4244.779	Ni II	32523.540	-3.11	
4246.82	4246.826	Sc II	2540.950	0.32	hfs 3 lines
4247.81	4247.805	Ti I	16106.075	-3.63	
4250.10	4250.119	Fe I	19912.594	-0.41	
4250.42	4250.437	Fe II	61974.931	-1.75	
4250.79	4250.787	Fe I	12560.933	-2.81	
4251.72	4251.717	Mn II	49882.153	-1.06	
4252.61	4252.632	Cr II	31117.390	-2.02	
4252.96	4252.962	Cr II	91955.392	-2.95	
	4252.963	Mn II	49889.858	-1.14	
4254.34	4254.336	Cr I	0.000	-0.11	
4254.51	4254.522	Cr II	47354.440	-0.97	
4258.15	4258.154	Fe II	21812.055	-3.40	
4258.33	4258.340	Fe II	21308.04	-4.13	
4259.19	4259.191	Si II	97972.086	-1.30	
4260.47	4260.474	Fe I	19350.891	-0.02	
4261.92	4261.913	Cr II	31168.581	-1.53	
4263.86	4263.869	Fe II	62049.023	-1.71	
4267.00	4267.001	C II	145549.272	0.61	
4267.25	4267.261	C II	145570.705	0.77	
4269.26	4269.277	Cr II	31082.940	-2.17	
4271.14	4271.153	Fe I	19757.031	-0.35	
4271.77	4271.760	Fe I	11976.238	-0.16	

Table 5—Continued

Corr. λ (Å)	Lab. λ (Å)	Ident.	E_{low} (cm $^{-1}$)	$\log(gf)$	Rem.
4273.32	4273.326	Fe II	21812.055	-3.26	
4274.78	4274.797	Cr I	0.000	-0.23	
4275.76	4275.779	Ti I	18825.781	-1.13	
4278.15	4278.159	Fe II	21711.917	-3.82	
4282.42	4282.403	Fe I	17550.180	-0.81	
4284.18	4284.188	Cr II	31082.940	-1.86	
4286.27	4286.280	Fe II	62171.614	-1.62	
4287.87	4287.872	Ti II	8710.440	-2.02	
4290.21	4290.219	Ti II	9395.710	-1.12	
4294.09	4294.099	Ti II	8724.250	-1.11	
4294.90	4294.91	Fe I	26351.038	-2.71	
4296.56	4296.572	Fe II	21812.055	-3.01	
4299.21	4299.206	Ti I	14106.633	-0.01	
4300.04	4300.049	Ti II	9518.060	-0.77	
4301.91	4301.914	Ti II	9363.620	-1.16	
4303.17	4303.176	Fe II	21812.055	-2.49	
4306.92	4306.916	Cr II	47372.533	-1.18	
4307.89	4307.863	Ti II	9395.710	-1.29	
4312.85	4312.864	Ti II	9518.060	-1.16	
4314.06	4314.076	Sc II	4987.790	-0.10	5 hfs lines
4314.29	4314.310	Fe II	21581.638	-3.48	
4314.97	4314.975	Ti II	9363.620	-1.13	
	4314.979	Fe II	38164.195	-3.10	
4318.16	4318.188	Fe II	63559.489	-1.98	
4319.40	4319.413	Fe II	61726.078	-2.12	
4319.67	4319.680	Fe II	63272.974	-1.76	
4320.34	4320.340	Ni II	113407.314	-2.72	
4320.72	4320.725	Sc II	4883.570	-0.26	
4320.93	4320.960	Ti II	9395.710	-1.97	
4321.32	4321.309	Fe II	63465.106	-1.83	
4324.97	4324.984	Sc II	4802.870	-0.44	2 hfs lines
4325.53	4325.540	Fe II	49100.978	-2.31	
	4325.523	Cr II	93276.860	-0.39	
4325.75	4325.762	Fe I	12968.554	-0.01	
4326.65	4326.639	Mn II	42537.180	-1.25	
4337.93	4337.915	Fe II	8710.440	-1.13	
4351.76	4351.769	Fe II	21812.055	-2.10	
4354.33	4354.344	Fe II	61726.078	-1.39	
4357.56	4357.584	Fe II	49100.978	-2.11	
4361.24	4361.247	Fe II	49506.935	-2.11	
4362.10	4362.099	Ni II	32499.529	-2.72	
4362.95	4362.924	Cr II	45669.369	-1.89	
4363.26	4363.255	Mn II	44899.820	-1.91	
4367.65	4367.659	Ti II	20891.660	-1.27	

Table 5—Continued

Corr. λ (Å)	Lab. λ (Å)	Ident.	E_{low} (cm $^{-1}$)	$\log(gf)$	Rem.
4368.24	4368.242	O I	76794.977	-2.03	
	4368.258	O I	76794.977	-2.25	
4369.39	4369.411	Fe II	22409.852	-1.67	
4383.54	4383.545	Fe I	11976.238	0.20	
4384.09	4384.094	Fe II	50212.823	-2.28	
4384.31	4384.319	Fe II	21430.359	-3.50	
4384.65	4384.637	Mg II	80619.500	-0.79	
4385.38	4385.387	Fe II	22409.852	-2.57	
4386.83	4386.844	Ti II	20951.620	-1.26	
4387.95	4387.930	He I	171134.897	-0.887	
4390.57	4390.514	Mg II	80650.022	-1.49	
	4390.572	Mg II	80650.022	-0.53	
4391.82	4391.791	Cr II	44307.091	-2.60	
	4391.820	S II	128233.197	-0.56	
4394.05	4394.051	Ti II	9850.900	-1.59	
4395.03	4395.033	Ti II	8744.250	-0.66	
4395.80	4395.817	Fe II	90487.811	-1.20	
4399.76	4399.772	Ti II	9975.920	-1.27	
4400.38	4400.379	Sc II	4883.570	-0.51	
4404.74	4404.75	Fe I	12560.933	-0.14	
4407.67	4407.678	Ti II	9850.900	-2.47	
4409.51	4409.516	Ti II	9930.690	-2.57	
4411.06	4411.07	Ti II	24961.031	-1.06	
4413.58	4413.601	Fe II	21581.638	-3.87	
4415.12	4415.122	Fe I	12968.554	-0.62	
4416.82	4416.830	Fe II	22409.852	-2.60	
4417.71	4417.719	Ti II	9395.710	-1.47	
4418.32	4418.330	Ti II	9975.920	-2.46	
4418.94	4418.957	Fe II	64087.418	-1.84	
4419.61	4419.604	Cr II	94365.189	-0.26	
4427.99	4427.994	Mg II	80619.500	-1.21	
4431.60	4431.605	Fe II	64040.884	-1.77	
4433.99	4433.988	Mg II	80650.022	-0.91	
4443.80	4443.794	Ti II	8710.440	-0.70	
4444.29	4444.299	Fe II	50157.455	-3.70	
4444.53	4444.539	Fe II	50157.455	-2.53	
4446.22	4446.237	Fe II	48039.087	-2.44	
4449.60	4449.616	Fe II	63948.792	-1.59	
4450.47	4450.482	Ti II	8744.250	-1.45	
4451.54	4451.551	Fe II	40506.935	-1.84	
4455.26	4455.266	Fe II	50512.823	-2.14	
4461.42	4461.439	Fe II	20830.582	-4.11	
4461.70	4461.706	Fe II	50212.823	-2.05	
4464.44	4464.450	Ti II	9363.620	-2.08	

Table 5—Continued

Corr. λ (Å)	Lab. λ (Å)	Ident.	E_{low} (cm $^{-1}$)	$\log(gf)$	Rem.
4468.49	4468.507	Ti II	9118.260	-0.60	
4471.48	4471.470	He I	169086.767	-2.212	
4471.48	4471.474	He I	169086.767	-1.036	
4471.48	4471.474	He I	169086.767	-0.287	
4471.48	4471.486	He I	169086.843	-1.035	
4471.48	4471.489	He I	169086.843	-0.558	
4472.92	4472.928	Fe II	22939.357	-3.43	
4476.01	4476.019	Fe I	22946.815	-0.97	
	4475.995	Fe II	90901.125	-1.03	
4478.64	4478.637	Mn II	53597.132	-0.95	
4480.71	4480.688	Fe II	50212.823	-2.39	
4481.12	4481.126	Mg II	71490.190	0.74	
	4481.150	Mg II	71490.190	-0.56	
4481.34	4481.325	Mg II	71491.064	0.59	
4487.48	4487.497	Fe II	62049.023	-2.14	
4488.31	4488.331	Ti II	25192.791	-0.82	
4489.17	4489.179	Ca II	68056.909	-0.61	
	4489.179	Ca II	68056.909	-0.61	
	4489.183	Ca II	22810.356	-2.97	
4491.40	4491.405	Fe II	23031.299	-2.70	
4493.52	4493.513	Ti II	8710.440	-2.73	
	4493.529	Fe II	63876.319	-1.43	
4494.54	4494.563	Fe I	17726.988	-1.14	
4501.26	4501.273	Ti II	8997.710	-0.75	
4507.09	4507.102	Fe II	62689.878	-1.92	
4508.27	4508.288	Fe II	23031.299	-2.21	
4511.77	4511.775	Cr II	52297.808	-1.37	
4512.02	4512.056	Fe II	61974.931	-2.18	
4515.32	4515.339	Fe II	22939.357	-2.48	
4515.59	4515.57	Cr II	67369.139	-1.11	
	4515.609	Fe II	50212.823	-1.11	
4518.33	4518.327	Ti II	8710.440	-2.55	
4520.21	4520.224	Fe II	22637.205	-2.60	
4522.63	4522.634	Fe II	22939.357	-2.03	3 Eu II hfs lines
4524.98	4524.997	Fe II	86124.299	-3.43	
4528.60	4528.614	Fe I	17550.180	-0.82	
4529.50	4529.474	Ti II	12676.970	-2.03	
	4529.569	Fe II	44929.549	-3.19	
4533.96	4533.969	Ti II	9975.920	-0.77	
4534.16	4534.168	Fe II	23031.299	-3.47	
4539.58	4539.595	Cr II	32603.400	-2.53	
4541.06	4541.058	Fe II	61973.931	-2.48	
4541.51	4541.524	Fe II	23031.299	-3.05	
4549.21	4549.192	Fe II	47674.718	-1.97	

Table 5—Continued

Corr. λ (Å)	Lab. λ (Å)	Ident.	E_{low} (cm $^{-1}$)	$\log(gf)$	Rem.
4549.47	4549.474	Fe II	22810.356	-1.75	
4549.62	4549.617	Ti II	12774.689	-0.45	
4552.40	4552.400	Cr II	93966.448	-4.09	
	4552.410	S II	121528.718	-0.10	
4553.63	4553.623	Cr I	31008.995	-3.95	
4554.03	4554.03	Ba II	0.000	0.02	15 hfs lines
4554.99	4554.988	Cr II	32836.680	-1.38	
4555.88	4555.893	Fe II	22810.356	-2.29	
4558.64	4558.650	Cr II	32854.311	-0.66	
4559.06	4559.079	Fe I	35379.205	-3.67	
4563.74	4563.761	Ti II	9850.900	-0.96	
4565.72	4565.74	Cr II	32603.400	-2.11	
4571.96	4571.968	Ti II	12676.970	-0.53	
4576.34	4576.340	Fe II	22939.357	-3.04	
4579.52	4579.527	Fe II	50212.823	-2.51	
4580.05	4580.063	Fe II	20830.582	-3.73	
4582.82	4582.835	Fe II	22939.357	-3.10	
4583.82	4583.837	Fe II	22637.205	-2.02	
4588.20	4588.199	Cr II	32836.680	-0.63	
4589.93	4589.958	Ti II	9975.920	-1.79	
4590.75	4590.736	Fe II	50187.813	-3.99	
4591.00	4591.004	Fe II	63272.974	-2.25	
4592.05	4592.049	Cr II	32854.949	-1.22	
4593.60	4593.606	Fe II	62049.023	-2.41	
4593.81	4593.827	Fe II	23317.632	-4.92	
4596.00	4596.015	Fe II	50212.823	-1.84	
4598.47	4598.494	Fe II	62945.040	-1.50	
4616.12	4616.124	Cr I	7927.443	-1.19	
4616.62	4616.629	Cr II	32844.760	-1.29	
4618.81	4618.803	Cr II	32854.949	-1.11	
4620.50	4620.521	Fe II	22810.356	3.28	
4621.40	4621.418	Si II	101023.046	-0.54	
4621.71	4621.696	Si II	101024.349	-1.68	
4625.89	4625.893	Fe II	48039.087	-2.20	
4628.76	4628.786	Fe II	63272.974	-1.74	
4629.32	4629.339	Cr II	22637.205	-2.37	
4631.87	4631.873	Fe II	63465.106	-1.87	
4364.07	4364.070	Cr II	32844.760	-1.24	
4635.30	4635.316	Fe II	48039.087	-1.65	
4638.04	4638.050	Fe II	62171.614	-1.52	
4640.80	4640.812	Fe II	62171.614	-1.88	
4648.93	4648.944	Fe II	20830.582	-4.39	
4656.97	4656.981	Fe II	23317.632	-3.63	
4663.05	4663.046	Al II	85481.348	-0.28	

Table 5—Continued

Corr. λ (Å)	Lab. λ (Å)	Ident.	E_{low} (cm $^{-1}$)	$\log(gf)$	Rem.
4663.70	4663.708	Fe II	23317.632	-4.27	
4665.55	4665.548	Ni II	55299.649	-1.82	
4666.75	4666.758	Fe II	22810.356	-3.33	
4670.16	4670.182	Fe II	20830.585	-4.10	
4673.28	4673.256	Si II	103556.025	-0.60	Broad
	4673.526	Si II	103556.025	-0.60	
4680.90	4680.904	Fe I	37162.745	-2.51	
4702.98	4702.991	Mg I	35051.263	-0.67	
4716.26	4716.271	S II	109831.595	-0.32	
4730.38	4730.395	Mn II	43339.420	-2.15	
4731.45	4731.453	Fe II	23317.632	-3.36	
4739.74	4739.709	Mg II	93311.112	-0.82	Broad
4755.73	4755.727	Mn II	43528.639	-1.24	
4764.72	4764.728	Mn II	43537.180	-1.35	
4771.73	4771.742	C I	60393.138	-2.12	
4779.98	4779.985	Ti II	16515.860	-1.37	
4805.09	4805.085	Ti II	16625.110	-1.10	
4812.35	4812.337	Cr II	31168.581	-1.80	
4815.56	4815.552	S II	110268.595	0.18	
4820.80	4820.834	Fe II	831366.488	-0.69	
4824.12	4824.127	Cr II	31219.350	-1.22	
4826.88	4826.888	Mn I	31076.421	-1.42	
4831.19	4831.202	Fe II	61041.746	-2.77	Broad
4833.20	4833.197	Fe II	21430.359	-4.78	
4836.22	4836.229	Cr II	31117.390	-2.25	
4848.25	4848.235	Cr II	31168.581	-1.14	
4864.31	4864.326	Cr II	31117.390	-1.37	
4871.30	4871.318	Fe I	23110.937	-0.41	
4872.11	4872.138	Fe I	21244.836	-0.60	
4873.46	4873.438	Ni I	29832.811	-0.47	
4874.02	4874.014	Ti II	24961.031	-0.79	
4876.41	4876.399	Cr II	31082.940	-1.46	
4883.28	4883.287	Fe II	82853.660	-0.64	
4884.600	4884.607	Cr II	31117.390	-2.08	
4890.76	4890.765	Fe I	23192.497	-0.43	
4891.48	4891.485	Cr II	31150.901	-3.04	
	4891.492	Fe I	22996.673	-0.14	
4893.82	4893.820	Fe II	22810.356	-4.45	
4901.60	4901.623	Cr II	52321.010	-0.83	
4908.15	4908.151	Fe II	83308.193	-0.30	
4911.19	4911.193	Ti II	25192.791	-0.34	
4912.45	4912.462	Cr II	52297.808	-0.95	
4913.29	4913.292	Fe II	82978.679	0.01	
4918.98	4918.994	Fe I	23110.937	-0.37	

Table 5—Continued

Corr. λ (Å)	Lab. λ (Å)	Ident.	E_{low} (cm $^{-1}$)	$\log(gf)$	Rem.
4920.49	4920.502	Fe I	22845.868	0.06	
	4921.931	HeI	171134.897	-0.443	
4921.99	4922.006	Ni II	112719.745	-0.60	
4923.92	4923.927	Fe II	23317.632	-1.32	
4925.34	4925.343	S II	109560.686	-0.24	
4948.06	4948.096	Fe II	83136.488	-0.32	
4948.77	4948.793	Fe II	83459.671	-0.01	
4951.57	4951.584	Fe II	83136.488	0.18	
4952.64	4952.657	Fe II	83459.671	-0.65	
4953.96	4953.987	Fe II	44929.549	-2.76	
4957.27	4957.298	Fe I	22996.673	-0.34	
4957.58	4957.596	Fe I	22650.414	0.13	
4958.82	4958.822	Fe II	82713.536	-0.65	
4967.89	4967.897	Fe I	33801.571	-0.53	
4968.81	4968.832	Fe I	33946.932	-2.57	
4977.02	4977.035	Fe II	83558.539	0.04	
4984.48	4984.488	Fe II	83308.193	0.01	
4990.50	4990.509	Fe II	83308.193	0.18	
4991.43	4991.440	Fe II	82853.660	-0.57	
4992.01	4992.024	Ni II	98822.511	0.99	
4992.35	4992.358	Cr II	47354.440	-4.78	
4999.17	4999.180	Fe II	82853.660	-0.48	
5000.72	5000.743	Fe II	22409.852	-4.74	
5001.48	5001.479	Ca II	60533.018	-0.52	
5001.94	5001.959	Fe II	82853.660	0.90	
5003.42	5003.414	Ni II	101144.633	0.70	
5004.19	5004.195	Fe II	82853.660	0.50	
5005.74	5005.742	Cr I	27728.811	-2.60	
5006.11	5006.119	Fe I	22845.868	-0.62	
5006.84	5006.841	Fe II	83713.536	-0.43	
5007.44	5007.447	Fe II	83726.362	-0.36	
5007.73	5007.739	Fe II	82978.679	-0.20	
5008.98	5009.022	Fe II ?	83459.671	-0.41	
5009.55	5009.567	S II	109831.595	-0.09	
5014.05	5014.042	S II	113461.537	0.03	
	5014.062	Ni II	100332.090	-0.70	
	5014.067	Cr II	84604.840	-2.14	
5014.95	5014.942	Fe I	31805.070	-0.25	
5015.73	5015.755	Fe II	83459.671	-0.05	Broad asymmetric
5018.44	5018.440	Fe II	23317.632	-1.22	
5021.56	5021.594	Fe II	82978.679	-0.30	
5022.41	5022.420	Fe II	83459.671	-0.06	
5022.78	5022.792	Fe II	82978.679	-0.02	
5026.79	5026.806	Fe II	83136.488	-0.22	

Table 5—Continued

Corr. λ (Å)	Lab. λ (Å)	Ident.	E_{low} (cm $^{-1}$)	$\log(gf)$	Rem.
5030.61	5030.630	Fe II	82978.679	0.40	
5031.01	5031.010	Sc II	10944.560	-0.26	
5031.88	5031.898	Fe II	83990.065	-0.78	
5032.42	5032.434	S II	110268.595	0.28	
5032.68	5032.712	Fe II	83812.317	0.11	
5035.69	5035.708	Fe II	82978.679	0.61	
5036.44	5036.427	Fe II	84359.799	-2.47	
5041.02	5041.024	Si II	81191.341	0.29	
5045.11	5045.114	Fe II	83136.488	-0.13	
5047.64	5047.641	Fe II	83136.488	-0.07	
5055.97	5055.984	Si II	81251.320	0.59	
5056.31	5056.317	Si II	81251.320	-0.36	
5056.70	5056.713	Cr II	69954.088	-1.68	
5058.38	5058.376	Ni II	10357.203	0.85	
5059.17	5059.20	Ni II	99132.784	0.54	
5060.24	5060.257	Fe II	84266.557	-0.52	
5061.70	5061.718	Fe II	83136.488	0.22	
5065.07	5065.097	Fe II	84131.564	-0.45	
5067.88	5067.893	Fe II	83308.193	-0.20	
5070.89	5070.899	Fe II	83136.488	0.24	
5072.00	5071.981	Fe II	90898.872	-1.62	
5072.27	5072.281	Ti II	25192.791	-0.75	
5074.05	5074.053	Fe II	54904.221	-1.97	
5075.76	5075.764	Fe II	84326.910	0.28	
5078.26	5078.296	Fe II	83990.065	-1.18	
5082.23	5082.230	Fe II	83990.065	-0.10	
5086.30	5086.306	Fe II	83990.065	-0.48	
5087.30	5087.303	Fe II	83713.536	-0.50	
5089.22	5089.214	Fe II	83308.193	-0.03	
5093.56	5093.576	Fe II	83713.536	0.11	triangular
5097.27	5097.271	Fe II	83713.536	0.31	
5100.71	5100.127	Fe II	83726.362	0.70	
5106.10	5106.097	Fe II	83812.317	-0.95	
	5106.109	Fe II	83308.193	-0.28	
5117.03	5117.034	Fe II	84131.564	-0.13	
5127.86	5127.866	Fe II	44929.549	-2.53	
5129.14	5129.152	Ti II	15257.430	-1.39	
5132.66	5132.669	Fe II	22637.205	-4.18	
5139.46	5139.462	Fe I	23711.453	-0.57	
5143.88	5143.880	Fe II	84266.557	0.10	
5144.34	5144.355	Fe II	84424.372	0.18	
5145.78	5145.772	Fe II	83990.065	-0.40	
5146.10	5146.127	Fe II	22810.356	-3.91	
5148.94	5148.907	Fe II	83990.065	-0.40	

Table 5—Continued

Corr. λ (Å)	Lab. λ (Å)	Ident.	E_{low} (cm $^{-1}$)	$\log(gf)$	Rem.
5149.46	5149.465	Fe II	84266.557	0.40	
5150.47	5150.489	Fe II	84266.557	-0.12	
5151.27	5151.247	Cr II	70316.899	-3.21	
5160.84	5160.839	Fe II	44915.046	-2.64	almost triangular
5163.58	5163.544	Fe II	84685.198	-1.90	
5165.69	5165.633	N I	94770.879	-2.18	broad Fe II 5165.649 ?
	5165.709	N I	94793.489	-3.35	Fe II 5165.751 ?
5166.55	5166.555	Fe II	84326.910	-0.03	triangular
5167.33	5167.321	Mg I	21850.405	-1.03	
5169.03	5169.033	Fe II	23317.632	-0.87	
5170.78	5170.777	Fe II	84326.910	-0.36	
5180.30	5180.314	Fe II	83812.317	0.04	
5185.53	5185.520	Si II	103556.025	-0.27	broad
	5185.555	Si II	103556.156	-0.39	
5185.88	5185.913	Ti II	15265.639	-1.35	
5186.85	5186.873	Fe II	84424.372	-0.30	
5188.67	5188.680	Ti II	12758.110	-1.21	
5191.43	5191.428	Cr II	30307.439	-3.36	
5192.35	5192.344	Fe I	24180.861	-0.42	
5193.72	5193.682	Fe II	93987.462	-3.30	
5194.38	5194.384	Fe II	179893.560	-3.21	
5194.89	5194.892	Fe II	84424.372	-0.15	
5197.56	5197.577	Fe II	26055.422	-2.10	
5199.11	5199.122	Fe II	83713.536	0.10	
5200.78	5200.804	Fe II	83812.317	-0.37	
5201.43	5201.468	Cr II	69954.088	-1.65	
5203.63	5203.638	Fe II	83812.317	-0.05	
5210.53	5210.539	Sc I	20236.860	0.43	
5213.98	5213.960	Fe II	84527.779	-0.22	
5215.34	5215.349	Fe II	83713.536	-0.01	
5215.81	5215.844	Fe II	83726.362	-0.23	
5216.85	5216.854	Fe II	84710.686	0.39	
	5216.863	Fe II	84527.779	0.61	
5218.85	5218.842	Fe II	83726.362	-0.21	
5222.36	5222.361	Fe II	84844.832	-0.33	
5223.24	5223.260	Fe II	83812.317	-0.41	
5223.80	5223.800	Fe II	83713.536	-0.59	
5224.40	5224.411	Fe II	83990.065	-0.57	
5225.34	5225.306	Cr II	86691.551	-0.66	
5226.00	5225.968	Fe II	83812.317	-0.41	
5226.54	5226.543	Ti II	12628.731	-1.30	
5227.48	5227.481	Fe II	84296.829	0.80	
5228.61	5228.648	Cr II	86078.899	-4.01	
5228.68	5228.695	Fe II	93487.649	-3.70	

Table 5—Continued

Corr. λ (Å)	Lab. λ (Å)	Ident.	E_{low} (cm $^{-1}$)	$\log(gf)$	Rem.
5232.49	5232.496	Cr II	32836.680	-2.09	
5232.77	5232.787	Fe II	83726.362	-0.06	
5232.94	5232.940	Fe II	23711.453	-0.19	
5234.29	5234.271	V II	18269.490	-4.42	
5234.62	5234.625	Fe II	25981.630	-2.05	
5237.32	5237.329	Cr II	32854.311	-1.16	
	5237.329	Cr II	86782.041	-0.58	
5239.80	5239.813	FeII	84326.910	-0.46	
5245.45	5245.455	Fe II	84326.910	-0.51	
5246.77	5246.768	Cr II	29951.880	-2.45	
5247.95	5247.952	Fe II	84938.177	0.63	
5249.39	5249.437	Cr II	30307.439	-2.43	
5251.23	5251.233	Fe II	84844.832	0.51	
5253.65	5253.641	Fe II	84296.829	-0.09	
5254.91	5254.929	Fe II	26055.422	-3.23	
5256.92	5256.938	Fe II	23317.632	-4.25	
5257.12	5257.122	Fe II	84685.198	0.03	
5260.24	5260.259	Fe II	84035.139	1.07	
5262.31	5262.317	Fe II	85048.600	-0.36	
5264.18	5264.177	Fe II	84710.686	0.36	
5264.79	5264.812	Fe II	26055.422	-3.19	
5272.39	5272.397	Fe II	48039.087	-2.03	
5274.96	5274.964	Cr II	32836.680	-1.29	
5275.98	5276.002	Fe II	25805.329	-1.94	
5278.91	5278.938	Fe II	47674.718	-2.41	
5279.87	5279.876	Cr II	32854.311	-2.10	
5280.05	5280.054	Cr II	32854.949	-2.01	
5284.09	5284.109	Fe II	23317.632	-3.19	
5291.65	5291.666	Fe II	84527.779	0.58	
5298.85	5298.860	Fe II	84844.832	-1.13	
5302.38	5302.402	Mn II	79569.268	0.23	
5303.40	5303.395	Fe II	66012.752	-1.61	
5305.85	5305.853	Cr II	30864.459	-2.36	
5306.17	5306.180	Fe II	84870.863	0.22	
5308.41	5308.408	Cr II	32836.680	-1.81	
5310.68	5310.687	Cr II	32844.760	-2.28	
5313.57	5313.563	Cr II	32854.949	-1.65	
5315.07	5315.086	Fe II	85048.600	-0.38	
5315.55	5315.563	Fe II	66377.284	-1.46	
5316.21	5316.225	Fe II	84035.139	0.34	
5316.77	5316.784	Fe II	25981.630	-2.91	
5318.06	5318.057	Fe II	84527.779	-0.14	
5318.74	5318.750	Fe II	84035.139	-0.57	
5322.23	5322.234	Fe II	84326.910	-0.52	

Table 5—Continued

Corr. λ (Å)	Lab. λ (Å)	Ident.	E_{low} (cm $^{-1}$)	$\log(gf)$	Rem.
5324.18	5324.179	Fe I	25899.986	-0.24	
5325.55	5325.553	Fe II	25981.630	-2.60	
5329.12	5329.096	O I	86625.757	-2.08	triplet
5329.70	5329.690	O I	86627.777	-1.41	
5330.76	5330.741	O I	86631.453	-1.12	
5334.86	5334.869	Cr II	32844.760	-1.56	
5336.78	5336.771	Ti II	12758.110	-1.70	broad
5337.74	5337.732	Fe II	26055.422	-3.89	
5339.59	5339.585	Fe II	84296.829	0.54	
5347.19	5347.190	Fe II	85172.810	-0.28	
5362.86	5362.869	Fe II	25805.329	-2.74	
5366.20	5366.207	Fe II	84710.686	-0.27	
5370.31	5370.309	Fe II	84710.686	-0.82	
5375.83	5375.827	Fe II	85048.600	-0.75	
	5375.847	Fe II	84296.829	-0.29	
5383.35	5383.369	Fe I	34782.420	0.50	
5387.04	5387.063	Fe II	84863.353	0.52	
5393.83	5393.847	Fe II	84296.829	-0.30	
5395.84	5395.857	Fe II	85495.303	0.36	
5401.60	5401.521	Mg II	93799.630	-0.45	triplet broad
	5401.556	Mg II	93799.750	-1.88	
	5401.556	Mg II	93799.750	-0.34	
5402.05	5402.059	Fe II	85184.734	0.50	
5404.14	5404.117	Fe I	34782.420	0.54	
	5404.151	Fe I	35767.561	0.52	
5405.07	5405.099	Fe II	85184.734	-1.01	
5405.71	5405.663	Fe II ?	84870.863	-0.44	
5407.62	5407.604	Cr II	30864.459	-2.09	
5408.80	5408.811	Fe II	48039.087	-2.39	
5414.05	5414.073	Fe II	25981.630	-3.79	
5414.85	5414.862	Cr II	55023.098	-1.78	
5415.19	5415.199	Fe I	35379.205	0.50	
5420.88	5420.922	Cr II	30307.439	-2.36	
5424.05	5424.068	Fe I	34843.954	0.52	
5425.24	5425.257	Fe II	25805.329	-3.36	
5427.80	5427.826	Fe II	54232.193	-1.66	
5428.66	5428.655	S II	109560.686	-0.01	
5429.96	5429.988	Fe II	85462.859	0.46	
5432.95	5432.967	Fe II	26352.767	-3.63	
5435.77	5435.775	O I	86627.777	-1.66	
5436.86	5436.862	O I	86631.453	-1.51	
	5436.868	Cr II	86980.102	-0.47	
5442.35	5442.351	Fe II	85048.600	-0.30	
5444.40	5444.387	Fe II	85495.303	-0.18	

Table 5—Continued

Corr. λ (Å)	Lab. λ (Å)	Ident.	E_{low} (cm $^{-1}$)	$\log(gf)$	Rem.
5445.79	5445.807	Fe II	85048.600	-0.11	
5450.07	5450.099	Fe II	85679.698	-0.53	
5453.83	5453.855	S II	110268.595	0.56	
5455.42	5455.454	Fe I	34843.954	0.30	
	5455.879	Cr II	33618.941	-3.00	
5455.90	5455.932	Fe II	84527.779	-0.52	
5457.73	5457.730	Fe II	85728.806	-0.17	
5465.93	5465.931	Fe II	85679.698	0.52	
5466.40	5466.461	Si II ?	101023.046	-0.20	
5466.89	5466.849	Si II	101024.349	-1.34	
	5466.894	Si II	101024.349	-0.04	
5473.59	5473.590	Fe II	85172.810	-0.79	
	5473.614	S II	109560.686	-0.12	
5475.81	5475.829	Fe II	84685.198	-0.18	
5478.36	5478.365	Cr II	33694.151	-1.91	
5479.40	5479.401	Fe II	85172.810	-0.41	triangular
5482.30	5482.308	Fe II	85184.734	0.43	
5487.62	5487.619	Fe II	85462.859	0.36	
5492.08	5492.079	Fe II	85679.698	-0.18	
5492.39	5492.399	Fe II	84685.198	-0.06	
5493.82	5493.833	Fe II	84685.198	0.21	
5502.08	5502.067	Cr II	33618.941	-1.99	
5502.67	5502.671	Fe II	85184.734	-0.14	
5503.21	5503.211	Fe II	84685.198	-0.09	
	5503.212	Cr II	33417.991	-2.31	
5506.18	5506.195	Fe II	84863.353	0.95	
5507.05	5507.072	Fe II	84870.863	-0.32	
5508.61	5508.606	Cr II	33521.110	-2.11	
5510.75	5510.779	Fe II	85184.734	0.00	
5525.12	5525.125	Fe II	26352.767	-4.61	triangular
5528.40	5528.405	Mg I	35051.263	-0.62	
5529.06	5529.053	Fe II	84870.863	-0.25	
5529.93	5529.932	Fe II	54273.640	-1.87	
5532.08	5532.088	Fe II	84870.863	-0.33	
5534.82	5534.847	Fe II	26170.181	-2.93	
5544.76	5544.763	Fe II	84863.353	0.12	
5549.00	5549.001	Fe II	84870.863	-0.23	
5554.93	5554.914	Fe II	85679.698	-0.64	
5567.84	5567.842	Fe II	54283.218	-1.89	
5577.94	5577.915	Fe II	85462.859	-0.14	
5586.77	5586.756	Fe I	27166.817	-0.21	
5587.08	5587.114	Fe II	54275.638	-2.18	
5588.21	5588.220	Fe II	85462.859	0.09	
5593.27	5593.300	Al II	106920.564	0.41	

Table 5—Continued

Corr. λ (Å)	Lab. λ (Å)	Ident.	E_{low} (cm $^{-1}$)	$\log(gf)$	Rem.
5606.14	5606.151	S II	110766.562	0.16	
5615.61	5615.644	Fe I	26874.547	-0.14	
5627.47	5627.458	Cr II	87858.560	0.21	
5640.32	5640.346	S II	110508.706	0.15	
5643.86	5643.880	Fe II	61726.078	-1.46	
5645.38	5645.392	Fe II	85184.734	0.08	
5648.90	5648.904	Fe II	85184.734	-0.24	
5657.91	5657.935	Fe II	27620.411	-4.10	
5658.18	5658.111	Ni II	53037.932	-2.15	
5658.79	5658.820	Fe II	85184.734	-0.72	
5659.98	5660.001	S II	110313.403	-0.07	
5691.00	5690.994	Fe II	86124.299	-0.20	
5716.50	5716.59	Fe II	62689.878	-2.26	broad
5726.55	5726.557	Fe II	86416.331	-0.02	
5747.87	5747.884	Fe II	44929.549	-2.91	
5780.13	5780.128	Fe II	86124.299	0.32	
5780.35	5780.336	Fe II	86416.331	-0.37	
5783.61	5783.630	Fe II	86416.331	0.21	
5784.43	5784.448	Fe II	86599.737	0.06	
5813.67	5813.677	Fe II	44929.549	-2.75	
5835.48	5835.492	Fe II	47674.718	-2.37	triangular
5854.19	5854.192	Fe II	86599.737	-0.19	
5875.10	5875.097	Fe II	87572.430	-2.36	
	5875.614	HeI	169086.766	-0.339	
	5875.615	HeI	169086.766	-0.409	
	5875.625	HeI	169086.843	-0.339	
	5875.640	HeI	169086.843	0.138	
5957.56	5957.559	Si II	81191.341	-0.30	
5978.93	5978.930	Si II	81251.320	0.00	
5990.97	5990.980	C I	69710.660	-3.58	
5991.36	5991.376	Fe II	25428.783	-3.56	
6071.38	6071.426	Fe II	86416.331	-0.19	
6084.09	6084.111	Fe II	25805.329	-3.81	
6103.49	6103.496	Fe II	50142.788	-2.17	triangular
6113.31	6113.322	Fe II	25981.630	-4.16	
6143.04	6143.026	Fe II	60956.779	-3.82	
6147.74	6147.741	Fe II	31364.440	-2.72	
6149.25	6149.258	Fe II	31368.450	-2.72	
6155.98	6155.961	O I	86625.757	-1.40	3 lines
6156.78	6156.778	O I	86627.777	-0.73	3 lines
6158.18	6158.187	O I	86631.453	-0.44	3 lines
6175.13	6175.146	Fe II	50187.813	-1.98	
6179.39	6179.384	Fe II	44915.046	-2.60	
6239.79	6231.750	Al II	105441.498	0.40	

Table 5—Continued

Corr. λ (Å)	Lab. λ (Å)	Ident.	E_{low} (cm $^{-1}$)	$\log(gf)$	Rem.
6238.39	6238.392	Fe II	31364.440	-2.63	
6239.62	6239.614	Si II	103556.025	0.19	3 lines
6239.93	6239.953	Fe II	31368.450	-3.44	
6243.40	6243.367	Al II	105470.928	0.67	
6247.55	6247.557	Fe II	31387.949	-2.33	
6347.09	6347.109	Si II	65500.472	0.30	broad
6371.35	6371.371	Si II	65500.472	0.00	broad
6402.23	6402.246	Na I	134041.838	0.36	
6416.92	6416.919	Fe II	31387.949	-2.74	